Research Article | Vol. 31, No. 3 / 30 Jan 2023 / Optics Express 4367
Optics EXPRESS

Suppression of coupling between optical aberration and tilt-to-length noise in a space-based gravitational wave telescope

HONGAN LIN,[1] JIANCONG LI,[1] YAOZHANG HUANG,[1] MIAO YU,[1] JIAXIONG LUO,[1] ZHI WANG,[2,3] AND YANXIONG WU[1,4,*]

[1] School of Physics and Optoelectronic Engineering, Foshan University, Foshan 528000, China
[2] Changchun Institute of Optics, Fine Mechanics, and Physics, Chinese Academy of Sciences, Changchun 1300033, China
[3] School of Fundamental Physics and Mathematical Sciences, Hangzhou Institute for Advanced Study, University of Chinese Academy of Sciences, Hangzhou 310124, China
[4] Ji Hua Laboratory, Foshan, Guangdong 528200, China
[*] wuyanxiong@fosu.edu.cn

Abstract: Coupling between exiting wavefront error of space gravitational wave telescopes and tilt-to-length (TTL) noise affects the measurement accuracy. Using the LISA Pathfinder signal, we analyzed cancellation and superposition of TTL coupling noise under various optical aberrations. We proposed proportion requirements of any two aberrations amplitude when noise was cancelled and an aberration amplitude control requirement when noise was superposed. Taking them as the aberration control requirements of gravitational wave telescope optical system, the exiting wavefront error requirements was reduced while suppressing the TTL coupling noise. A 40× optical telescope system with detection aperture φ=200 mm was designed. The exiting wavefront error was relaxed from 0.02 λ to 0.0496 λ. The maximum coupling coefficient value did not exceed 6.9448 pm/μrad within a pointing jitter angle of ±300 μrad. The proposed approach should be useful in future telescope design.

1. Introduction

In 2016, the Laser Interferometer Gravitational-Wave Observatory (LIGO) detected a gravitational wave generated by the merging of two black holes and, thus, confirmed Einstein's prediction made one century before this incident [1–3]. Despite this success, LIGO's ability to detect gravitational radiation is hampered by low-frequency Earth pulse vibrations, gravitational gradient noise, and the Earth's curvature. A space-based gravitational wave detection system can overcome these limitations. The most sensitive detection band of this system lies in the range of 0.1 mHz–1 Hz [4]. To accurately detect the gravitational waves, the measurement noise of the observatory in this detection band must be lower than $1\text{pm}/\sqrt{Hz}$. This imposes strict requirements on all parts of the observatory [5].

It is particularly important to ensure optical path stability and wavefront quality of the optical telescope—the device that transmits and receives signals at the front end of the gravitational wave detector [6,7] with picometer precision. However, in space laser interferometry, satellites are vulnerable to nonconservative forces generated in the space environment, resulting in tilt-to-length (TTL) noise caused by the tilt of the beam received by the telescope [8]. According to existing research findings, the influence of TTL noise on laser interferometry can be suppressed by adding an imaging system in front of the quadrant photodiode (QPD) [9]. However, TTL noise can still couple with the wavefront error owing to the telescope's manufacturing and processing characteristics; this coupling is an important noise source that affects the accuracy of interferometry [10]. Based on the present guidelines, the coupling coefficient should not exceed

#480537 https://doi.org/10.1364/OE.480537
Journal © 2023 Received 11 Nov 2022; revised 31 Dec 2022; accepted 3 Jan 2023; published 23 Jan 2023

25 pm/μrad within the range of the pointing jitter angle of ±300 μrad [11]. It is conducive to reduce the sensitivity of optical path length information to telescope jitter, which decreases the additional optical path length introduced in heterodyne interferometry, improves the analytical accuracy of interferometry, and restores a more complete gravitational-wave signal [12].

In recent years, there has been considerable progress toward the suppression of the influence of TTL coupling noise on the accuracy of space laser interferometry. Sasso *et al.* considered the wavefront error composed of the first eight Zernike polynomials and calculated the relationship between pointing jitter and low-order aberration coupling based on the analysis of the LISA Pathfinder (LPF) signal; they found that the root-mean-square (RMS) value of the telescope's wavefront error should be less than λ/65 to meet the detection requirements [13,14]; Zhao *et al.* considered the first 25 Fringe Zernike polynomials to fit the exit pupil wavefront of the telescope and demonstrated that the wavefront error RMS value of the LPF signal should be less than λ/50 to meet the detection criteria [15,16]. However, published studies have neither thoroughly explored the coupling mechanism between optical aberrations and TTL noise nor proposed specific control requirements for the amplitudes or ratios between different aberrations in the telescope optical system; therefore, strict control requirements for the exiting wavefront error remain necessary.

Accordingly, we aimed to effectively relax the control requirements of wavefront errors when the coupling coefficient meets the requirements. First, we studied the influence of different aberrations on TTL noise and developed a theory on the cancellation and superposition of different optical aberrations coupled with TTL noise. Subsequently, we obtained a ratio of aberration amplitudes, for which the coupling coefficient is almost completely canceled. Regarding the superposition relationship, we proposed additional control requirements for the aberration that contributes the most to TTL coupling noise in superposition cases. Further, we regarded this as the aberration control requirement of the optical system of the gravitational wave telescope, which effectively reduces the control requirement of the exit pupil's wavefront telescope error and thus decreases the difficulty of the design of the optical system. This study demonstrates that the coupling coefficient for the same system's wavefront error is reduced significantly after the inclusion of these cancellation and superposition control requirements. When the RMS value of the wavefront error was λ/20, which is 2.5 times wider than the RMS value required to meet the detection criteria in current practice, the control requirements of the coupling coefficient of the space gravitational wave detection were met. Finally, according to the theoretical research and analysis efforts outlined above, an optimized optical space-based gravitational wave telescope system was designed, which provides an effective reference for subsequent optical system's designs of telescopes.

2. Optical model

The space-based gravitational wave telescope intercepts and shrinks the far field wavefront into a flat-top beam, then transmits this signal to the optical platform, where it interferes with the local Gaussian beam on the QPD, as shown in Fig. 1. Assuming that the centers of the two interference beams coincide, the phase information O_{ovi} is obtained by integrating over the QPD surface [10],

$$O_{ovi} = \int_S E_1 E_2^* dr^2 = \int_S e^{\frac{-r^2}{\omega(z)^2}} e^{ikW(r,\theta)} dr^2, \tag{1}$$

where E_1 and E_2 represent the Gaussian and flat-top beams, respectively; (r, θ) are the polar coordinates of the detector surface; $\omega(z)$ is the spot size on the detector, and $W(r, \theta)$ is the total wavefront error of the system.

Because of the inevitable pointing jitter of the telescope, TTL noise will be introduced and coupled with the telescope wavefront error, which is an important source of noise that affects the accuracy of interferometry. To describe more directly the coupling relationship between TTL

Optics EXPRESS

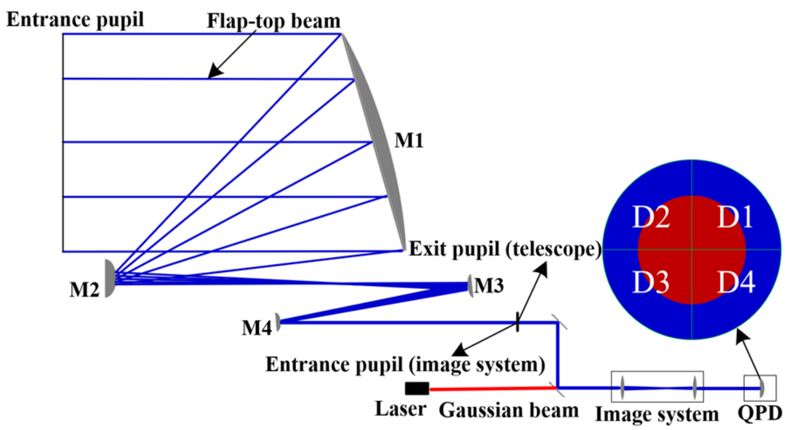

Fig. 1. Optical path system of a space laser interferometer (QPD: quadrant photodiode).

noise and wavefront error, and to identify a method to suppress TTL coupling noise, we use the Fringe Zernike polynomials to fit the telescope wavefront error signal [15]. In addition to the radial symmetric defocus (DE) and two spherical aberration terms, the sinusoidal and cosine terms of other Zernike aberrations are combined to represent the vector form of aberrations, as shown in Table 1.

Table 1. Aberration consisting of Fringe Zernike polynomials

i	*n, m*	*j*	$Z_j(\rho, \theta)$	Aberration name
2,3	1,±1	1	$2\rho\cos(\theta - \theta_{TI})$	Tilt
4	2,0	2	$\sqrt{3}(2\rho^2 - 1)$	Defocus (DE)
5,6	2,±2	3	$\sqrt{6}\rho^2 cos(2\theta - \theta_{\mathrm{PA}})$	Primary astigmatism (PA)
7,8	3,±1	4	$\sqrt{8}(3\rho^2 - 2\rho)\cos(\theta - \theta_{\mathrm{PC}})$	Primary coma (PC)
9	4,0	5	$\sqrt{5}(6\rho^4 - 6\rho^2 + 1)$	Primary spherical (PS)
10,11	3,±3	6	$\sqrt{8}\rho^3\cos(3\theta - \theta_{PTR})$	Primary trefoil (PTR)
12,13	4,±2	7	$\sqrt{10}(10\rho^5 - 12\rho^3 + 3\rho)\cos(2\theta - \theta_{\mathrm{SA}})$	Secondary astigmatism (SA)
14,15	5,±1	8	$\sqrt{12}(10\rho^5 - 12\rho^3 + 3\rho)\cos(\theta - \theta_{\mathrm{SC}})$	Secondary coma (SC)
19,20	5,±3	11	$\sqrt{12}(5\rho^5 - 4\rho^3)\cos(3\theta - \theta_{\mathrm{STR}})$	Secondary trefoil (STR)

The LPF signal was used to calculate the phase information to determine the optical path noise. The coupling coefficient (δ) is the first derivative of the LPF optical path noise with respect to the tilt angle, and its expression is given as,

$$\delta = B_1 + 2 * B_2 * \alpha, \tag{2}$$

where the detailed derivation process of Eq. (2) is presented in Supplement 1, α is the inclination angle of the laser, and the coefficients B_1 and B_2 are respectively expressed as,

$$B_1 = v_1 * M_1 * v_2^T, \tag{3}$$

$$B_2 = v_2 * M_2^T, \tag{4}$$

$$v_1 \Rightarrow \{C_4^{\mathrm{PC}}, C_8^{\mathrm{SC}}, C_6^{\mathrm{PTR}}, C_{11}^{\mathrm{STR}}\}, \tag{5}$$

$$v_2 \Rightarrow \{A_2^{\mathrm{DE}}, A_5^{\mathrm{PS}}, B_3^{\mathrm{PA}}, B_7^{\mathrm{SA}}\}, \tag{6}$$

where v_1 is an aberration vector with the components given in Eq. (5), namely, the amplitudes of the primary coma (PC), secondary coma (SC), primary trefoil (PTR), and secondary trefoil (STR),

Optics EXPRESS

and v_2 is another vector comprising the amplitudes of DE, primary spherical (PS) aberration, primary astigmatism (PA), and secondary astigmatism (SA). The components of matrices M_1 and M_2 are given in Tables 2 and 3; they represent the constant terms obtained after the addition of Zernike polynomials, which are the coefficient matrices obtained by setting the normalized radius to $\omega_r = 1$ and setting both θ_{TI} and θ_{aber} to 0. Thus, Eq. (2) demonstrates that there is no relationship between the coma and the trefoil terms that are both independently coupled with TTL and that the spherical aberration and DE are not coupled with the trefoil. For the convenience of subsequent analyses, the aberration amplitudes in v_1 and v_2 will be denoted as A_j^{aber}, B_j^{aber}, and C_j^{aber}, where the term "aber" indicates the abbreviation of different aberrations and j = 1, 2, 3, . . . , 11 indicates the serial number of the aberration.

Table 2. M_2 matrix

a \ b, $M_1(a,b)$	1 (DE)	2 (PS)	3 (PA)	4 (SA)
1 (PC)	-12266.0	-8789.6	-2226.4	-11292.0
2 (SC)	3362.6	-12382.0	924.2	-4108.0
3 (PTR)	0	0	-12324.0	-1334.9
4 (STR)	0	0	2190.5	-12018

Table 3. M_2 matrix

b	1 (DE)	2 (PS)	3 (PA)	4 (SA)
M_2(b)	-5098000	-1319400	-5772800	1210800

According to the coupling of different types of optical aberrations with TTL noise, the two terms in Eq. (2) were separated and were then summarized as follows according to the characteristics of the analytical formula:

$$\begin{aligned}\delta_1 &= 2*B_2*\alpha \\ &= M_2(\mathrm{b})*A_j^{aber}*\alpha + M_2(b)'*B_j^{aber}*\alpha*\cos(\theta_{aber}-2\theta_\alpha),\end{aligned} \tag{7a}$$

$$\begin{aligned}\delta_2 &= B_1 \\ &= M_1(a,b)*A_j^{aber}*C_j^{aber}*\cos(\theta_{aber}-\theta_\alpha) \\ &+ M_1(a,b)'*B_j^{aber}*C_j^{aber}*\cos(\theta_{aber}-\theta_{aber}-\theta_\alpha),\end{aligned} \tag{7b}$$

where Eq. (7a) is an analytical formula used for coupling an aberration vector with TTL noise and Eq. (7b) is an analytical formula for coupling two aberration vectors with TTL noise. The $M_1(a, b)$ and $M_2(b)$ are the relevant components of coefficient matrices M_1 and M_2. We analyzed Eqs. (7a) and (7b) and determined that effective suppression can be obtained with a $\delta \le 25$ pm/μrad aberration control requirement.

3. Effect of aberration on TTL coupling noise

3.1. Cancellation relationship between optical aberration and TTL noise after coupling

The different optical aberrations at the exit pupil of the telescope have different characteristics after coupling with TTL noise; this can lead to partial cancellation instead of a single superposition relationship between various aberrations and the TTL noise after coupling. This section starts with the theory on the influence of aberration on TTL noise coupling in the cancellation relationship, and analyzes the reason for the formation of cancellation relationship.

Optics EXPRESS

First, we expanded and divided Eq. (7a) into Eqs. (8a)–(8d),

$$\delta_1^{\mathrm{DE}} = 5.0980 * 10^6 * A_2^{\mathrm{DE}} * \alpha, \tag{8a}$$

$$\delta_1^{PS} = -1.3194 * 10^6 * A_5^{\mathrm{PS}} * \alpha, \tag{8b}$$

$$\delta_1^{\mathrm{PA}} = -5.7728 * 10^6 * B_3^{\mathrm{PA}} * \alpha * \cos(\theta_{PA} - 2\theta_\alpha), \tag{8c}$$

$$\delta_1^{\mathrm{SA}} = 1.2108 * 10^6 * B_7^{\mathrm{SA}} * \alpha * \cos(\theta_{\mathrm{SA}} - 2\theta_\alpha). \tag{8d}$$

Thus, four wavefronts containing only DE, PS, PA, or SA were generated respectively, and each generated wavefront was substituted into the corresponding Eqs. (8a)–(8d) for calculation. Figures 2(a), 2(b), 2(d), and 2(e) show the four results obtained when the coupling coefficient was ±25 pm/μrad. Combined with the analytical formula and the corresponding TTL coupling noise calculation results, the coefficients of Eqs. (8a) and (8b) for circularly symmetric aberrations (DE and PS) have opposite signs, the noise results were circularly symmetric, and the noise directions in the middle and edge regions between them were opposite. Accordingly, we incorporated both into Eq. (7a) for simultaneous calculation, and found that the final coupling coefficient was canceled, i.e., its value was extremely small (6.56×10^{-5} pm/μrad), as shown in Fig. 3(c). In addition, by simultaneously adding the amplitudes B_3^{PA} and B_7^{SA} of centrosymmetric aberration to Eq. (7a), the coupling coefficient was canceled again. As shown in Fig. 2(f), the noise results were centrosymmetric and both exhibited opposite characteristics in the x and y directions. Therefore, controlling aberration amplitudes with opposite characteristics can lead to cancellation after coupling with TTL noise.

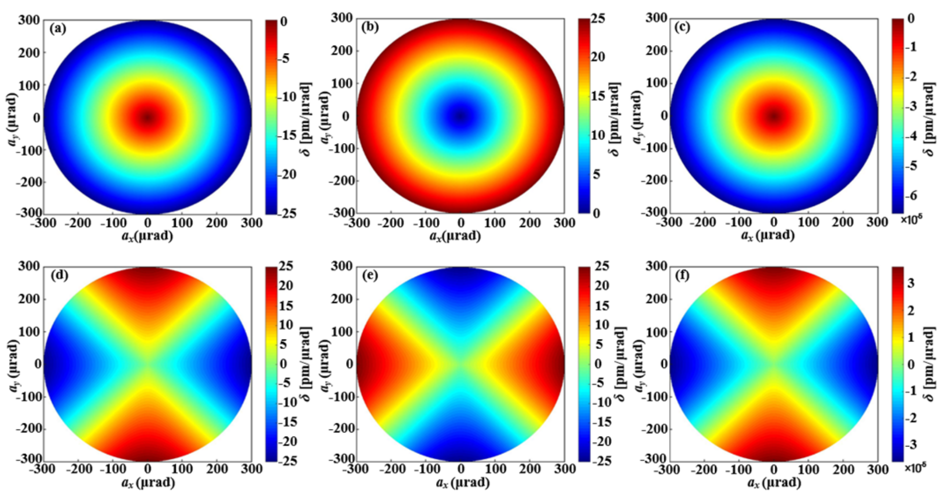

Fig. 2. Tilt-to-length coupled noise calculation results for various aberration amplitudes: (a) $A_2^{\mathrm{DE}} = 0.01635\lambda$. (b) $A_5^{\mathrm{PS}} = 0.06316\lambda$. (c) $A_2^{\mathrm{DE}} = 0.01635\lambda$ and $A_5^{\mathrm{PS}} = 0.06316\lambda$. (d) $B_3^{\mathrm{PA}} = 0.01444\lambda$. (e) $B_7^{\mathrm{SA}} = 0.06882\lambda$. (f) $B_3^{\mathrm{PA}} = 0.01444\lambda$ and $B_7^{\mathrm{SA}} = 0.06882\lambda$.

Further, to describe the cancellation mechanism after the coupling of aberration and TTL noise more intuitively, we plotted the variation of the coupling coefficient as A_2^{DE} and A_5^{PS}, varying in the range of 0–0.01 λ. As shown in Fig. 3(a), with the increase in A_2^{DE} or A_5^{PS}, the coupling coefficient first decreased and then increased. When the ratio of the two equaled to the slope of the red straight line, the coupling coefficient was at its minimum and was almost completely canceled. In addition, we found that, when only DE and TTL noise were coupled, the coupling coefficient reached a maximum. Similarly, when we set the variation range of B_3^{PA} and B_7^{SA} to 0–0.01 λ and

Optics EXPRESS

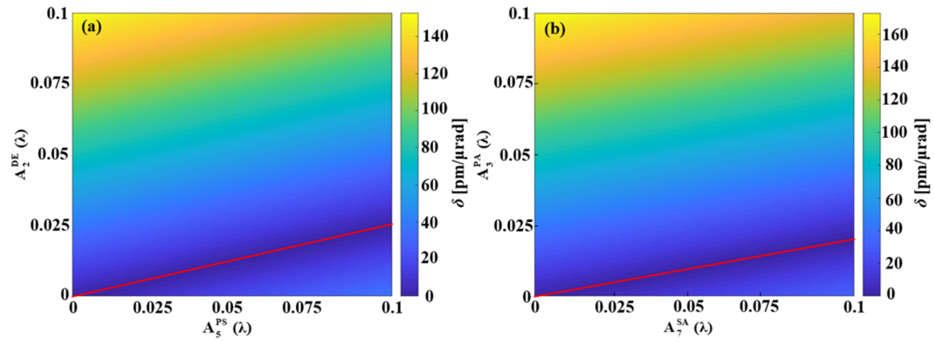

Fig. 3. Tilt-to-length coupled noise changing with aberration amplitudes A_j^{aber}. (a) A_2^{DE} and A_5^{PS}. (b) B_3^{PA} and B_7^{SA}.

obtained the results of the coupling coefficient variation with B_3^{PA} and B_7^{SA}, the position at which the coupling coefficient reached its minimum value was also along the red straight line, as shown in Fig. 3(b). Therefore, the slope of the red line is the aberration cancellation ratio. When the ratio between aberrations reaches the cancellation ratio, the influence of TTL coupling noise on spatial interferometry is suppressed to the maximum.

To evaluate this ratio, Eqs. (8a), (8b), (8c), and (8d) of the corresponding aberrations were combined to obtain the best cancellation ratios, namely, $A_5^{\mathrm{PS}}/A_2^{\mathrm{DE}} = 3.864$ and $B_7^{\mathrm{SA}}/B_3^{\mathrm{PA}} = 4.768$. When these conditions are fulfilled, the coupling coefficient is approximately equal to 0 and the tilt-to-length coupled noise can be suppressed to the greatest extent.

The values of A_2^{DE} in Fig. 2 obeying the optimal cancellation ratio were inserted simultaneously into Eq. (7a). The result is shown in Fig. 4(b). Coupling coefficients less than 1×10^{-5} pm/μrad were far lower than the control requirements of the coupling coefficient in space-based gravitational wave detection. In addition, based on the cancellation ratio, the worst cases in which the detection requirements were met were obtained, which had opposite noise directions (Figs. 4(a) and 4(c)). Thus, controlling the ratio between the canceled aberrations is an effective approach to suppress the TTL coupling noise such that the wavefront errors at the same level can have lower coupling coefficients.

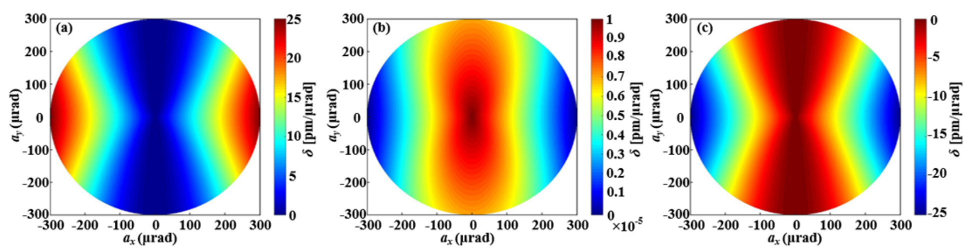

Fig. 4. Tilt-to-length coupled noise calculation results meeting the detection requirements: (a) and (c) worst results; (b) best results.

3.2. Superposition relationship between optical aberration and TTL noise after coupling

As discussed in the previous section, effective suppression of the TTL coupling noise was achieved by controlling the ratio of canceling aberrations to achieve the best canceling ratio. However, only the DE, PS, PA, and SA amplitudes were considered. There are other optical aberrations in the wavefront of the actual telescope optical system. These aberrations have a

Optics EXPRESS

superposition relationship with the TTL noise after coupling. By adding the control requirements to the superposition aberrations, the TTL coupling noise can also be suppressed effectively.

We continued to use the aberration amplitudes A_2^{DE}, A_5^{PS}, B_3^{PA}, and B_7^{SA} shown in Fig. 2 by adding C_4^{PC}, C_8^{SC}, C_6^{PTR}, and C_{11}^{STR}, respectively, to analyze the influence of coma and trefoil terms on the TTL noise. In the analysis, the influence of Eq. (7a) on the TTL coupling noise can be ignored because the amplitude of the canceling aberration reaches the canceling ratio. Here, only the partial expansion of Eq. (7b) was considered, and an analytical formula for the coupling of TTL noise with two different aberrations was obtained as follows:

$$\begin{aligned}\delta_2 =& M_1(1,1)^* A_2^{\mathrm{DE}} * C_4^{\mathrm{PC}} * \cos(\theta_{\mathrm{PC}} - \theta_\alpha) \\ &+ M_1(2,1) * A_2^{\mathrm{DE}} * C_8^{\mathrm{SC}} * \cos(\theta_{\mathrm{SC}} - \theta_\alpha) \\ &+ M_1(1,3) * B_3^{\mathrm{PA}} * C_4^{\mathrm{PC}} * \cos(\theta_{\mathrm{PA}} - \theta_{\mathrm{PC}} - \theta_\alpha) \\ &+ M_1(2,3) * B_3^{\mathrm{PA}} * C_8^{\mathrm{SC}} * \cos(\theta_{\mathrm{SC}} - \theta_{\mathrm{PA}} + \theta_\alpha).\end{aligned} \tag{9}$$

According to Eq. (9), the value of the coupling coefficient depends on the aberration amplitude, coefficient, and cosine term. For the convenience of subsequent analyses, we did not consider the direction angle of aberration, i.e., θ_{aber} was set to 0. In the M_1 matrix, the only components of M_1 with positive coefficient symbols were $M_1(2, 1)$, $M_1(2, 3)$, and $M_1(4, 3)$; most components had negative coefficient symbols. Additionally, when the spherical and astigmatism terms reached the cancellation ratio, $M_1(2,1) \times A_2^{\mathrm{DE}} \times C_8^{\mathrm{SC}} << M_1(2,2) \times A_5^{\mathrm{PS}} \times C_8^{\mathrm{SC}}$, $M_1(2,3) \times B_3^{\mathrm{PA}} \times C_8^{\mathrm{SC}} << M_1(2,4) \times B_7^{\mathrm{SA}} \times C_8^{\mathrm{SC}}$, and $M_1(4,3) \times B_2^{\mathrm{PA}} \times C_{11}^{\mathrm{STR}} << M_1(4,4) \times B_7^{\mathrm{SA}} \times C_{11}^{\mathrm{STR}}$. Therefore, δ_2 could be represented by the same symbol, and the distribution of TTL coupling noise maintained the same direction and resulted in the superposition of the coupling coefficient with the addition of coma and trefoil terms. As shown in Fig. 5(a), the calculation result included four canceling aberrations plus a specific aberration coupled with TTL noise and the amplitude of the specific aberration was equal to 0.015947 λ. For ease of comparison, Fig. 5 shows all four calculation results using color bars at the same scale; the largest coupling coefficient was obtained after the addition of PC (±25 pm/μrad). The coupling coefficients calculated by adding trefoil (Figs. 5(c) and (d)) were close to 0. Based on this superposition principle, controlling the amplitudes of the coma and trefoil terms can effectively suppress the TTL coupling noise. However, considering the difficulty of the design, we only controlled the aberration with the highest contribution.

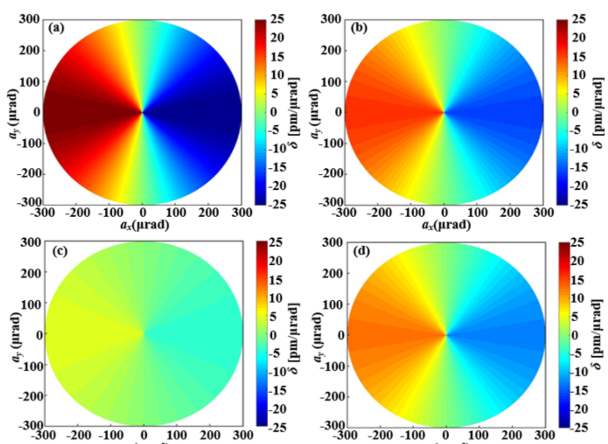

Fig. 5. Tilt-to-length coupled noise calculation results for various aberration amplitudes: (a) $C_4^{\mathrm{PC}} = 0.01597\lambda$, (b) $C_8^{\mathrm{SC}} = 0.01597\lambda$, (c) $C_6^{\mathrm{PTR}} = 0.01597\lambda$, and (d) $C_{11}^{\mathrm{STR}} = 0.01597\lambda$.

To analyze the contribution of coma and trefoil terms to the TTL coupling noise, the variation ranges of C_4^{PC}, C_8^{SC}, C_6^{PTR}, and C_{11}^{STR} were all set in the range of 0–0.01 λ. As shown in Fig. 6, the coupling coefficient increased as a function of the aberration amplitude, but PC contributed the most toward the TTL coupling noise, whereas PTR contributed the least. Therefore, it is more important to control the value of the PC than that of the SC, PTR, and STR in the optical system's design of space-based gravitational wave telescopes.

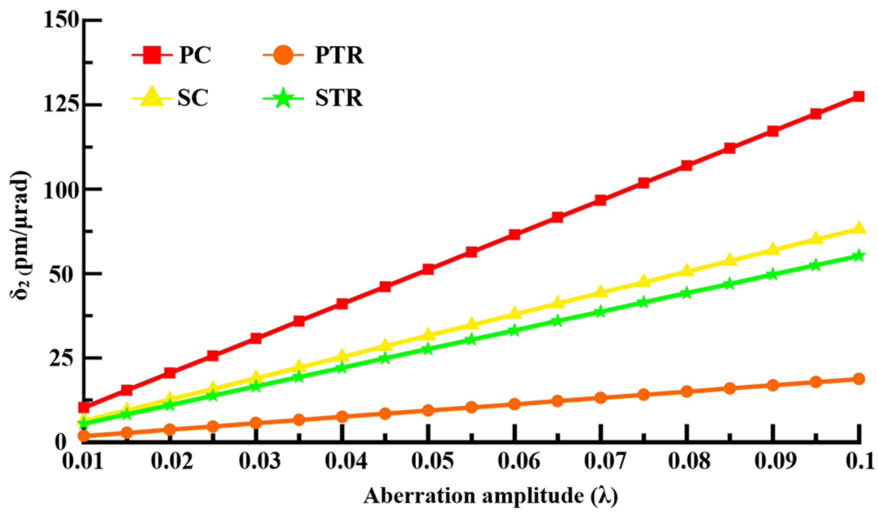

Fig. 6. Contributions of primary coma (PC), secondary coma (SC), primary trefoil (PTR), and secondary trefoil (STR) to the tilt-to-length coupling noise coefficient δ_2 as a function of aberration amplitude.

Focusing on the index of the TTL coupling noise, we separated Eq. (9), in which PC was coupled with other aberration terms, and established the following control requirement for PC:

$$A_4^{\mathrm{PC}} \leq \left| \frac{25}{-\ 1.1528 * 10^4 {*} A_2^{\mathrm{DE}} - 2.0925 * 10^3 {*} A_5^{\mathrm{PS}} - 8.2609 * 10^3 {*} B_3^{\mathrm{PA}} - 1.0613 * 10^4 {*} B_7^{\mathrm{SA}}} \right|. \tag{10}$$

The TTL coupling noise can be reduced further by incorporating this control requirement into the design of the optical system.

3.3. Noise cancellation and superposition theory reduces the limiting effect of the telescope's wavefront error

We used the Monte Carlo algorithm to predict the coupling of wavefront error with TTL noise at the exit pupil of the telescope at different constraints in the following two cases: 1) when there are no restrictions on aberration and 2) when the ratio of circularly symmetric and centrally symmetric aberration is controlled and the amplitude of PA is controlled according to Eq. (9).

For the control system's total wavefront error RMS values were equal to λ/50, λ/40, λ/30, λ/20, and λ/10, 10,000 samples meeting the abovementioned aberration control requirements and wavefront errors were randomly generated by the Monte Carlo algorithm and inserted into Eq. (3). The parameters θ_{aber} and higher-order aberrations were not considered in the calculations; α was used to replace θ_{Ti}, and the maximum value of the TTL coupling noise was obtained within the range of ±300 μrad.

The results of the analysis are shown in Fig. 7. To compare the analyzed results at different aberration control requirements, we list the maximum values of the coupling coefficients at

Optics EXPRESS

different aberration control requirements and wavefront errors together with the proportion of samples which did not exceed 25 pm/μrad in Table 4. The coupling coefficient distribution for any wavefront error RMS value was smaller in case (1) than that in case (2). Additionally, when the RMS value was λ/20, the proportion of samples meeting the coupling coefficient requirements reached 99.77%, whereas the proportion of samples in case (2) was only 6.04%. In addition, it is worth noting that the coupling coefficient was relatively large in case (1). Herein, we considered the worst case, in which the amplitude of superposed aberrations at the exit pupil of the telescope was very large and the coupling between these aberrations and noise lad to a higher coupling coefficient.

Table 4. Maximum value of the coupling coefficient and percentages of values below 25 pm/μrad at different control requirements

Case	λ/50		λ/40		λ/30		λ/20		λ/10	
	Maximum (Max)	proportion	Max	proportion	Max	proportion	Max	proportion	Max	proportion
Case 1	4.271	100.00%	6.63	100.00%	11.69	100.00%	26.70	99.77%	104.47	7.89%
Case 2	41.21	87.10%	51.40	63.42%	66.68	30.51%	104.67	6.04%	231.97	0.00%

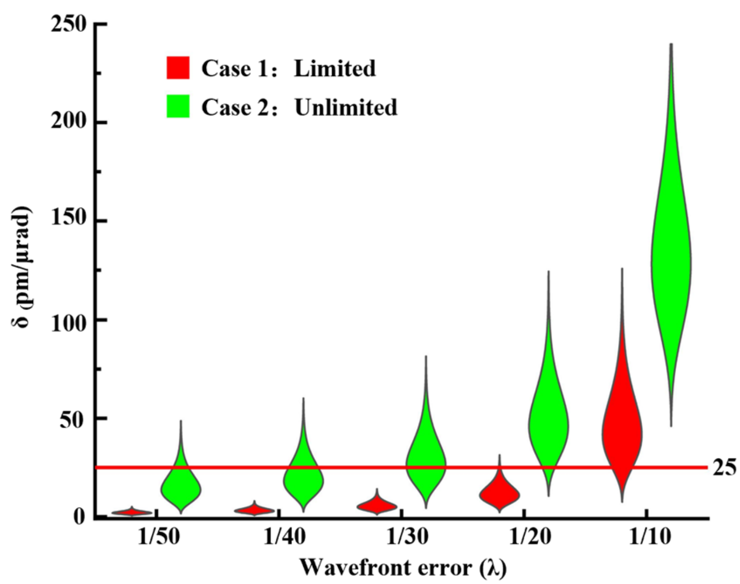

Fig. 7. Coupling effect of different numerical wavefront errors and tilt-to-length noise in cases of unlimited and limited aberrations. The red line indicates the critical coupling coefficient level (25 pm/μrad).

Therefore, in designing the optical system for a space-based gravitational wave telescope, it is necessary to control the proportion of canceled aberrations and the amplitude of the superposed aberrations. This can effectively relax the control requirements of the wavefront quality at the exit pupil of the telescope while suppressing the TTL coupling noise.

4. Optimal design of the telescope optical system

The space-based gravitational wave telescope should not only meet basic imaging quality requirements but also meet the measurement requirements such that the coupling coefficient does not exceed 25 pm/μrad. Achieving this noise level by using previously published methods requires imposing higher restrictions on the wavefront error, thus increasing the design difficulty and manufacturing costs. However, by using the proposed law of cancellation and superposition of coupling coefficients between aberrations to relax the control requirements of the wavefront error while meeting those of the coupling coefficient as the final evaluation index, we can reduce the design difficulty by providing the optimal design for an off-axis, defocused, four-mirror optical system. The design index of the optical telescope system is shown in Table 5.

Table 5. Optical system design index

Parameter	System Requirement
Exit pupil diameter	200 mm
Wavelength	1064 nm
Field-of-view	±8 μrad
Afocal magnification	40×
Coupling coefficient	≤25 pm/μrad

We controlled the aberration amplitudes to reach the cancellation ratios ($A_5^{\mathrm{PS}}/A_2^{\mathrm{DE}}$= 3.864, $B_7^{\mathrm{SA}}/B_3^{\mathrm{PA}}$= 4.768). By controlling the amplitude of PC according to Eq. (9) and by establishing the RMS value of the wavefront error of the telescope system to be equal to λ/20, the optical system of the space-based gravitational wave telescope can be optimized, as shown in Fig. 8. The design indices of each reflector of the telescope are listed in Table 6. The amplitude ($A_{\mathrm{j}}^{\mathrm{aber}}$, $B_{\mathrm{j}}^{\mathrm{aber}}$, $C_{\mathrm{j}}^{\mathrm{aber}}$) and direction angle ($\theta_{\mathrm{j}}$) of the optical aberration of the telescope system are listed in Table 7. As shown in Fig. 9, the wavefront error of the telescope system was 0.0496 λ. The ratio of DE to PS was 3.864 and that of PA to SA was 4.768, both of which meet the aberration cancellation ratio requirements. As a result of coupling between the wavefront error and TTL noise, the maximum coupling coefficient value does not exceed 6.9448 pm/μrad within a pointing jittering angle range of ±300 μrad, which meets the noise requirement.

Table 6. Optimized design parameters of the space-based based gravitational wave telescope's optical system

Mirror	Radius (mm)	Thickness (mm)	Conic	Decenter Y (mm)	Tilt (°)
PM	-1064.226	-508.412	-0.876	-120	0
SM	-49.924	574.0562	2.272	0	0
TM	-723.420	-245.658	0	-5	-1.5
QM	756.211	246.871	0	-7	-0.5

Table 7. Zernike polynomial fitting of the amplitude and direction of the wavefront at the exit pupil of the telescope

$A_{\mathrm{j}}^{\mathrm{aber}}(B_{\mathrm{j}}^{\mathrm{aber}}, C_{\mathrm{j}}^{\mathrm{aber}})/\theta_{\mathrm{j}}$	A_2^{DE}	$B_3^{\mathrm{PA}}/\theta_{\mathrm{PA}}$	$C_4^{\mathrm{PC}}/\theta_{\mathrm{PC}}$	A_5^{PS}	$C_6^{\mathrm{PTR}}/\theta_{\mathrm{PTR}}$
nm/rad	4.12	3.82/0	27.48/0	15.93	33.46/-1.57
$A_{\mathrm{j}}^{\mathrm{aber}}(B_{\mathrm{j}}^{\mathrm{aber}}, C_{\mathrm{j}}^{\mathrm{aber}})/\theta_{\mathrm{j}}$	$B_7^{\mathrm{SA}}/\theta_{SA}$	$C_8^{\mathrm{SC}}/\theta_{SC}$	A_9^{SS}	$A_{10}^{\mathrm{PTE}}/\theta_{PTE}$	$C_{11}^{\mathrm{STR}}/\theta_{STR}$
nm/rad	18.19/0	5.14/-1.57	0.36	0.74/0	0.44/-1.57

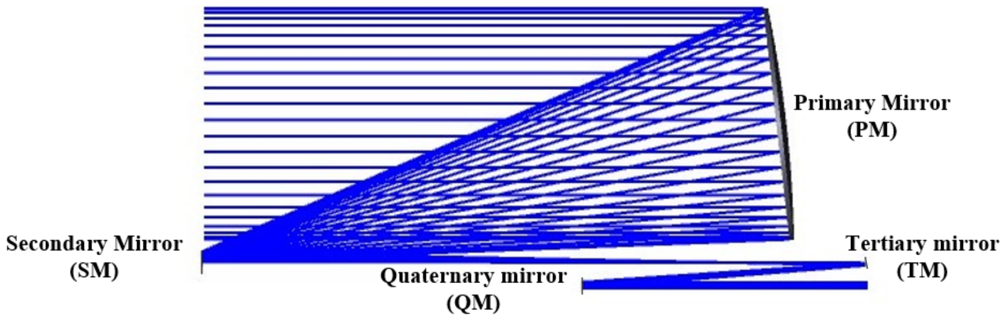

Fig. 8. Optimized optical system of the space-based gravitational wave telescope.

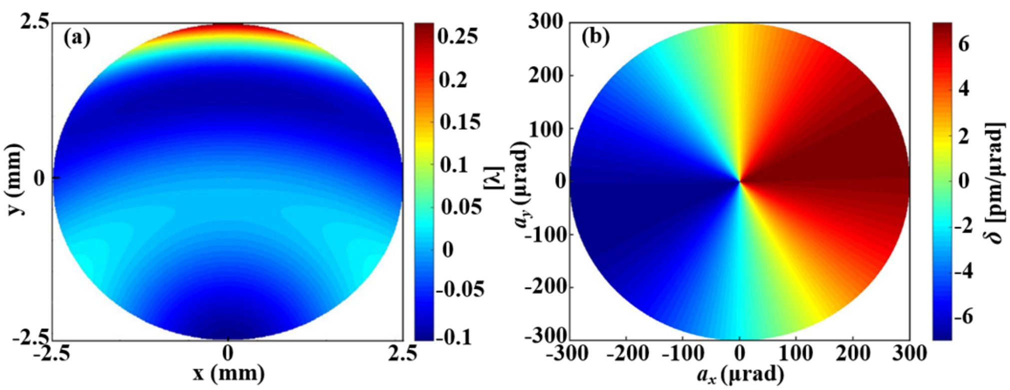

Fig. 9. (a) Wavefront at the exit pupil of the optimized telescope. (b) Calculated tilt-to-length coupled noise.

5. Conclusion

In this study, we evaluated the influence of optical aberration on TTL noise using the LPF signal and investigated the theory associated with the cancellation and superposition after the coupling of optical aberration with TTL noise. We inferred that, when the ratio of PS aberration to DE was 3.864 and that of PA to SA was 4.768, TTL coupling noise was suppressed to the greatest extent. Control requirements were proposed for PC aberration, which contributes the most to TTL coupling noise in the superposed aberration. With these aberration control requirements, the detection requirements could be met with a wavefront error RMS value of λ/20, which is 2.5 times wider than that required currently.

Based on this analysis, the optimal design for a space-based gravitational wave telescope was proposed. The ratio of canceling aberration was approximately equal to the optimal aberration, and the amplitude of superposed aberration met the control requirements. The maximum value of the coupling coefficient did not exceed 6.9448 pm/μrad within the ±300-μrad pointing jitter range, and the RMS value of the total wavefront error of the system was relaxed to 0.0496 λ. These results provide an effective reference for subsequent research on suppressing TTL coupling noise, thus leading to an improved design for space-based gravitational wave telescopes.

Funding. National Natural Science Foundation of China (No. 62075214); Science and Technology Planning Project of Guangdong Province (No. X190311UZ190); Research and development projects in key areas of Guangdong Province (No. 2020B1111040001).

Disclosures. The authors declare no conflicts of interest.

Data availability. No data were generated or analyzed in the presented research.

Optics EXPRESS

Supplemental document. See Supplement 1 for supporting content.

References

1. K. Belczynski, D. E. Holz, T. Bulik, and R. O'Shaughnessy, "The first gravitational wave source from the isolated evolution of two 40-100 M_{sun} stars," Nature **534**(7608), 512–515 (2016).
2. B. P. Abbott, R. Abbott, T. D. Abbott, M. R. Abernathy, F. Acernese, K. Ackley, C. Adams, T. Adams, P. Addesso, R. X. Adhikari, V. B. Adya, C. Affeldt, M. Agathos, K. Agatsuma, N. Aggarwal, O. D. Aguiar, L. Aiello, A. Ain, P. Ajith, B. Allen, L. I. G. O. Scientific Collaboration, and V. Collaboration, "Observation of gravitational waves from a binary black hole merger," Phys. Rev. Lett. **116**(6), 061102 (2016).
3. Z. Luo, S. Bai, X. Bian, G. Chen, P. Dong, Y. Dong, W. Gao, X. Gong, J. He, H. Li, X. Li, Y. Li, H. Liu, and M. Shao, "Gravitational wave detection by space laser interferometry," Adv. Mech. **43**(4), 415–447 (2013).
4. A. Sutton, K. McKenzie, B. Ware, and D. A. Shaddock, "Laser ranging and communications for LISA," Opt. Express **18**(20), 20759–20773 (2010).
5. D. R. Weise, P. Marenaci, P. Weimer, H. R. Schulte, P. Gath, and U. Johann, "Alternative opto-mechanical architectures for the LISA instrument," J. Phys.: Conf. Ser. **154**, 012029 (2009).
6. J. C. Livas, P. Arsenovic, J. A. Crow, P. C. Hill, J. M. Howard, L. T. Seals III, and S. Shiri, "Telescopes for space-based gravitational wave missions," Opt. Eng **52**(9), 091811 (2013).
7. A. L. Verlaan, H. Hogenhuis, J. Pijnenburg, M. Lemmen, S. Lucarelli, D. Scheulen, and D. Ende, "LISA telescope assembly optical stability characterization for ESA," Proc. SPIE **10564**, 845003–174 (2012).
8. S. Schuster, G. Wanner, M. Tröbs, and G. Heinzel, "Vanishing tilt-to-length coupling for a singular case in two-beam laser interferometers with Gaussian beams," Appl. Opt. **54**(5), 1010–1014 (2015).
9. M. Chwalla, K. Danzmann, M. D. Álvarez, J. J. E. Delgado, G. Fernández Barranco, E. Fitzsimons, O. Gerberding, G. Heinzel, C. J. Killow, M. Lieser, M. Perreur-Lloyd, D. I. Robertson, J. M. Rohr, S. Schuster, T. S. Schwarze, M. Tröbs, G. Wanner, and H. Ward, "Optical suppression of tilt-to-length coupling in the LISA long-arm interferometer," Phys. Rev. Applied **14**(1), 014030 (2020).
10. Y. Zhao, J. Shen, C. Fang, H. Liu, Z. Wang, and Z. Luo, "Tilt-to-length noise coupled by wavefront errors in the interfering beams for the space measurement of gravitational waves," Opt. Express **28**(17), 25545–25561 (2020).
11. M. Chwalla, K. Danzmann, G. Fernández Barranco, E. Fitzsimons, O. Gerberding, G. Heinzel, C. J. Killow, M. Lieser, M. Perreur-Lloyd, D. I. Robertson, S. Schuster, T. S. Schwarze, M. Tröbs, H. Ward, and M. Zwetz, "Design and construction of an optical test bed for LISA imaging systems and tilt-to-length coupling," Class. Quantum Grav. **33**(24), 245015 (2016).
12. S. Chen, C. Wang, H. Jiang, H. Sun, and Z. Tao, "Reducing phase noise coupled by wavefront errors in optical telescopes for the space measurement of gravitational waves," Opt. Express **30**(21), 37648–37663 (2022).
13. C. P. Sasso, G. Mana, and S. Mottini, "Coupling of wavefront errors and pointing jitter in the LISA interferometer: misalignment of the interfering wavefronts," Class. Quantum Grav. **35**(24), 245002 (2018).
14. C. P. Sasso, G. Mana, and S. Mottini, "Telescope jitters and phase noise in the LISA interferometer," Opt. Express **27**(12), 16855 (2019).
15. Y. Zhao, J. Shen, C. Fang, Z. Wang, R. Gao, and W. Sha, "The far-field optical path noise coupled with the pointing jitter in the space measurement of gravitational waves," Appl. Opt. **60**(2), 438–444 (2021).
16. C. Fang, "AO.nb," Optica Publishing Group, software, figshare (2021), https://doi.org/10.6084/m9.figshare.12800657.v1